Periodic density functional theory study of the crystal morphology of $FeZn_{13}$

Weihua Zhu, Hong Mei Jin, Ping Wu,* and Hong Lin Liu
Institute of High Performance Computing, 1 Science Park Road, #01-01 The Capricorn, Singapore Science Park II, Singapore 117528
(Received 8 April 2004; published 27 October 2004)

A periodic DFT total energy calculation has been performed to investigate the crystal morphology of the $FeZn_{13}$ surfaces by using slab model. The effects of the slab thickness, the vacuum width between slabs, and the surface relaxation on surface energy have been tested. The results show that the vacuum width of 6 Å and the slab thickness of 23.5 Å are enough to obtain meaningful results. Relaxation effect on the surface structure is small. The order of the morphological importance predicted at the DFT level is $(200)>(020)>(110)>(001)>(11\bar{1})>(20\bar{1})>(201)>(111)$. We also present comparisons of the crystal morphology predicted by the BFDH, attachment energy and surface energy method at empirical and DFT level. The calculated surface energy anisotropies are then applied to the determination of the equilibrium shape of $FeZn_{13}$.

DOI: 10.1103/PhysRevB.70.165419 PACS number(s): 68.55Jk, 68.35.Bs, 31.15.Ar

I. INTRODUCTION

The generation of zinc and zinc alloy coatings on steel is one of the most important processing techniques used to protect steel components exposed to corrosive environments. Typical processing methods used in producing zinc coatings include hot-dip galvanizing, thermal spraying and electrodeposition. Recently, a considerable amount of research has occurred on the hot-dip galvanizing process and on new types of zinc coatings because of new applications in the automotive and building industries.[1] The galvanized structure is usually made of Zn-Fe intermetallic alloy layers, which are composed of zeta, delta, $gamma_1$ and gamma phases.[1] The most widely accepted iron-zinc equilibrium phase diagram presented by Kubachewski and Massalski[2] shows that the outermost phase of zinc coatings is the zeta (ζ) phase, $FeZn_{13}$. The zeta phase layer is capable of growing epitaxially on the substrate alpha (α) iron at an extremely high rate,[3] and may exert significant influence on the following phase growth. In the field of crystal growth, one of the central problems of interest is the prediction of crystal morphology from the internal crystal structure. Consequently, the understanding of the morphology of the $FeZn_{13}$ phase is of great important to predict and control microstructures of galvanized coatings. As the precise nature of the $FeZn_{13}$ morphology is not known there is a clear need to gain an understanding of that at the atomic level.

An initial approach of morphological prediction was based solely on the lattice-plane spacings of different crystal faces.[4] The growth rate of the face is inversely proportional to its interplanar spacing. Donnay and Harker[5] refined this approach by developing rules that related the crystal symmetry to the possible growth planes. This method is an approximation based on geometrical considerations. Later, the attachment energy method[6] and the surface energy method[7] were proposed to predict crystal morphology. Various empirical techniques based on interatomic potentials have been used to calculate attachment energy and surface energy. These calculations highly depend on the quality of the interatomic potentials; moreover it is difficult to adjust an interatomic potential functional form and parameters which are able to incorporate both a covalent and an ionic character for the bonds existing in the real systems in order to obtain a genuine realistic description. However, an alternative approach, first-principles techniques, which have no fitting parameters and are transferable in various local bonding environments, can eliminate these drawbacks as the interatomic potentials are directly computed from the electronic structure.

This work is a part of our research on zinc coatings by using computer simulation.[8–10] Here we perform periodic density functional theory (DFT) total energy calculations to study the morphology of the $FeZn_{13}$ surfaces by using the slab model. Particular emphasis is placed on the technical aspects of the calculations. These include the slab thickness, the vacuum width between slabs, the surface relaxation and the comparison of DFT results with empirical method calculations. Then we investigate the morphology of several low-index $FeZn_{13}$ surfaces. Finally the equilibrium shape of $FeZn_{13}$ is found using the Wulff construction.

II. COMPUTATIONAL METHOD

A. Computational details

Our calculations performed in this study within the framework of DFT were done using the Vienna *ab initio* simulation package VASP and the ultrasoft pseudopotential database contained therein.[11–14] The interaction between ions and electrons is described by fully nonlocal optimized ultrasoft pseudopotentials similar to those introduced by Vanderbilt.[15,16] These pseudopotentials allow a smaller basis set for a given accuracy. The residual minimization technique[13,14] is used to calculate the electronic ground state. The relaxation of different atomic configures is based on a conjugate-gradient (CG) minimization[11] of the total energy. The generalized gradient approximation (GGA) proposed by Perdew and Wang,[17,18] named PW91, is employed. The *k*-points are obtained from the Monkhost-Pack scheme.

The degree of total energy convergence depends on the plane-wave cutoff and the density of *k*-point sampling within

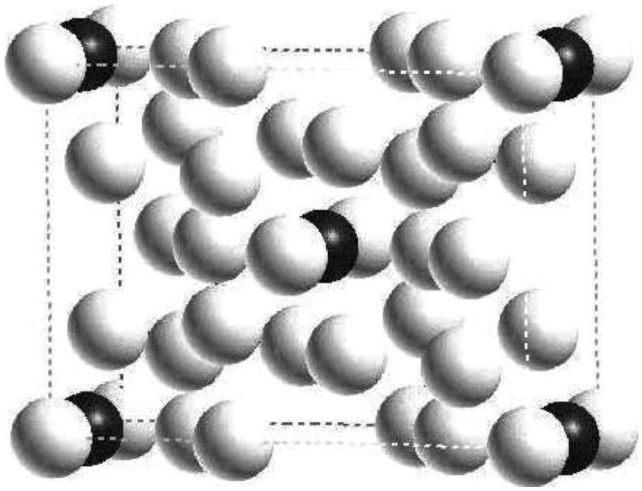

FIG. 1. The unit cell of $FeZn_{13}$ compound derived from Refs. 19–22. Light spheres are zincs and dark spheres are irons.

the Brillouin zone. We have investigated these by undertaking a number of calculations for one-layer slab with different values for these parameters. When the kinetic energy cutoff is changed from 400 eV to 500 eV, the total energy is converged to within 0.01 eV at a grid of $4\times4\times1$. With the energy cutoff of 400 eV, changing the *k*-point grids from $4\times4\times1$ to $5\times5\times1$ gave a change in the total energy of less than 0.003 eV. Therefore, a cutoff energy of 400 eV and a grid of $4\times4\times1$ have been used for the following calculations.

To model the $FeZn_{13}$ surface at periodic boundary conditions, a slab of finite thickness perpendicular to the surface but infinite extension in the other two directions is used. Slabs are separated from repeated replicas by a certain vacuum width. The thickness of the slabs is usually expressed in terms of a number of layers, where one layer is defined as the depth of one unit cell that contains 2 iron and 26 zinc atoms. These slab surfaces were obtained by cleaving $FeZn_{13}$ crystal whose structure was first reported by Brown[19] and then refined by others.[20–22] Bulk $FeZn_{13}$ has a monoclinic unit cell and contains an iron atom and a zinc atom surrounded by 12 zinc atoms as the vertices of slightly distorted icosahedron, shown in Fig. 1. The lattice parameters of the $FeZn_{13}$ crystal are as follows: $a=10.862$ Å, $b=7.608$ Å, $c=5.061$ Å, $\alpha=\gamma=90°$, $\beta=100.52°$.

B. Methods of morphology prediction

Three methods may be used to predict the external morphology of crystalline materials from the internal crystal structure: the Brevais-Friedel-Donnay-Harker (BFDH) method, the attachment energy method and the surface energy method. The BFDH method is a geometrical calculation that uses the crystal lattice and symmetry to generate a list of possible growth faces and their relative growth rates.[4,5] From this, crystal morphology can be deduced. The method is an approximation, and does not account for the energetics of the system.

The attachment energy method can predict the shape of the crystal more accurately because it takes the energetics of the system into account. The attachment energy E_{att} is computed as:[23]

$$E_{att} = E_{latt} - E_{slice}, \tag{1}$$

where E_{latt} is the lattice energy of the crystal, and E_{slice} energy released on the formation of a growth slice of thickness d_{hkl}. The growth rate of the crystal face is proportional to its attachment energy. That is, faces with the lowest attachment energies are the lowest growing, and, therefore, have the most morphological importance. The morphology derived by this methodology is known as the growth morphology since it is based on the idea of layers attaching themselves to a growing crystal.

Another method to crystal morphology is via the surface energy. The surface energy is calculated from the difference in energy of the surface ions to those in the bulk per unit surface area:

$$E_{surf} = (E_{slab} - nE_{bulk})/A, \tag{2}$$

where E_{surf} is the surface energy, E_{slab} is the total energy per repeated slab supercell, E_{bulk} is the energy per unit cell in the bulk, n is the number of unit cells, and A is the total surface area per repeated unit. For a crystal in equilibrium with its surroundings, the surface energy must be minimal for a given volume. Hence the morphological importance of a face is inversely proportional to the surface energy.[24] The morphology derived in this way is termed the equilibrium morphology.

According to above knowledge of three methods, the relative growth rate R is defined as:

$$R = X(hkl)/X(h'k'l'), \tag{3}$$

where $X(hkl)$ and $X(h'k'l')$ stand for center-to-face distance D, attachment energy E_{att} or surface energy E_{surf} for the faces of Miller indexes (hkl) and $(h'k'l')$, respectively. Thus, faces with the lowest relative growth rate have the most morphological importance.

In this work, our main purpose is to perform periodic density functional theory total energy calculations to study the morphology of the $FeZn_{13}$ surfaces by using slab model. For comparison, we also list the crystal morphology predicted by the BFDH, attachment energy and surface energy method at empirical level using the Cerius2 software.[25]

III. RESULTS AND DISCUSSION

A. Bulk properties of $FeZn_{13}$

In order to benchmark the accuracy of the method for our surface calculations, we carried out initial tests on the bulk $FeZn_{13}$ system. The full relaxation of the structure was performed to allow the ionic configurations, cell shape and volume to change. We compared relaxed lattice parameters and atomic fractional coordinates for $FeZn_{13}$ unit cell with experimental results in Table I. It is found that the calculated results are in good agreement with experimental values. These comparisons confirm that our computational parameters are reasonably satisfactory.

TABLE I. Comparison of relaxed lattice parameters (Å) and atomic fractional coordinates for $FeZn_{13}$ unit cell with experimental results.

	DFT relaxation			Experiment[a]		
	a	*b*	*c*	*a*	*b*	*c*
	10.817	7.530	5.164	10.862	7.608	5.061
	u	*v*	*w*	*u*	*v*	*w*
Fe	0.000	0.000	0.500	0.000	0.000	0.500
Zn	0.000	0.000	0.000	0.000	0.000	0.000
Zn	0.615	0.000	0.290	0.611	0.000	0.292
Zn	0.223	0.000	0.069	0.220	0.000	0.073
Zn	0.076	0.293	0.834	0.077	0.292	0.835
Zn	0.175	0.181	0.552	0.176	0.178	0.545

[a]References 19 and 20.

B. Convergence tests for slab surface supercells

Here the surface energy method is applied to measure the stability of the surfaces. As a compromise between computational efficiency and accuracy, only the (110) surface is considered as an example for these tests. To ensure that the results of the calculation accurately represent an isolated surface, we have tested the convergence of vacuum width and slab thickness.

Figure 2 presents the variation of surface energy as a function of vacuum width for slab thicknesses of 2 and 3 layers. With increasing vacuum width, the evolution pattern of surface energy for slab thicknesses of 2 and 3 layers is very similar. The vacuum width has a marked effect on the surface energy for vacuum widths smaller than 2.0 Å, but a small effect for vacuum widths larger than 2.0 Å. The differences in the surface energy of slab thicknesses of 2 and 3 layers are very small for vacuum widths larger than 2.0 Å. This shows that slab thicknesses of 2 and 3 layers have a small effect on their surface energy. Therefore, the vacuum width of 6 Å is enough to obtain meaningful results. In all subsequent calculations, vacuum widths of 10.0 Å are used.

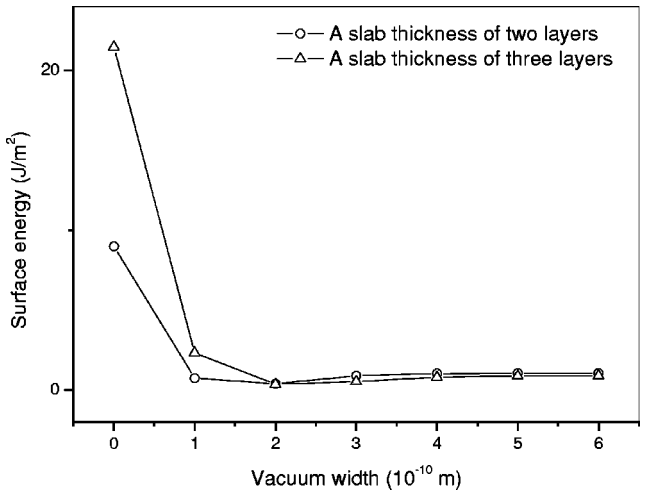

FIG. 2. The variation of surface energy as a function of vacuum width for slab thicknesses of 2 and 3 layers.

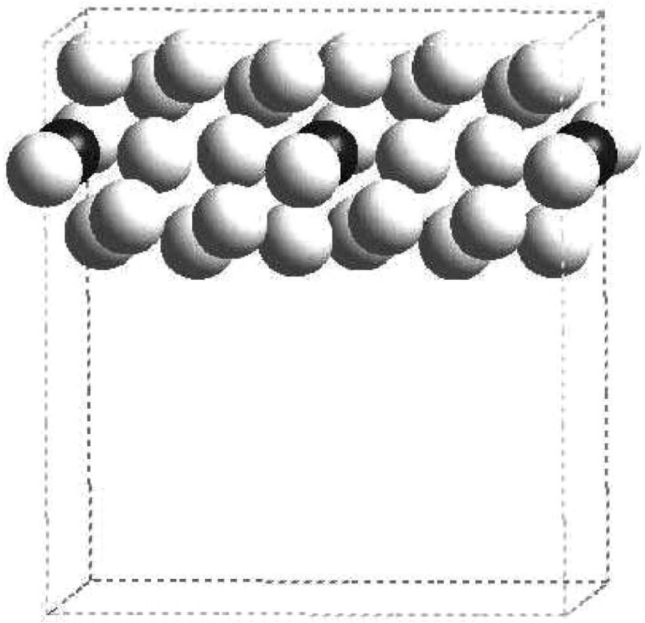

FIG. 3. The $FeZn_{13}$ (110) surface of one-layer slab. Light spheres are zincs and dark spheres are irons.

We performed two kinds of relaxation ways: to relax ions only; to relax both ions and cell shape. All the ions in slab unit cell are allowed to relax. The selection of one-layer slab (2 Fe and 26 Zn atoms), as shown in Fig. 3, in relaxation calculations was balanced against computational cost. Table II compares the relaxed lattice parameters with unrelaxed ones for the slab surface of one-layer thickness. It is seen that the calculated values for the lattice parameters are in agreement with unrelaxed results. This shows that relaxation of the slab surface has a small effect on the crystal structure. We compared relaxed atomic fractional coordinates for slab face of one-layer thickness with unrelaxed results in Table III. The relaxed atomic fractional coordinates under two kinds of relaxation ways change very small, compared with unrelaxed values. This agrees with the observation that the relaxation of high symmetry surfaces in relatively close-packed metallic systems is small.[26] Thus only ions were allowed to relax in the following relaxation calculations.

Figure 4 displays the evolution of surface energy with the increment of slab thickness under unrelaxation and relaxation. The calculated results show that the slab thickness has a small effect on the surface energy at first, but convergence to the infinite limit is rapid. This observation is inconsistent with previous studies on the TiO_2 surface.[27] Considering the relaxation effects, the variation trend of the surface energy with increment of slab thickness is similar to the unrelaxed results after four-layer slabs. Since the relaxation calcula-

TABLE II. Comparison of relaxed lattice parameters with unrelaxed results for one-layer slab surface.

	a(Å)	*b*(Å)	*c*(Å)
Unrelaxed	5.061	13.261	14.821
Relaxed	5.327	13.409	15.243

TABLE III. Comparison of atomic fractional coordinates under relaxation of both ions and cell shape or only ions with unrelaxed results for one-layer slab surface.

Atom	Unrelax results			Relax ions and cell shaps			Relax ions only		
	u	v	w	Δu	Δv	Δw	Δu	Δv	Δw
Fe	0.6186	0.0000	0.8077	0.0057	−0.0074	0.0233	0.0061	−0.0051	0.0108
Fe	0.6186	0.5000	0.8077	0.0058	−0.0073	0.0232	0.0061	−0.0052	0.0110
Zn	0.1186	0.0000	0.8077	0.0137	0.0021	−0.0094	0.0108	0.0015	−0.0071
Zn	0.1186	0.5000	0.8077	0.0137	0.0021	−0.0094	0.0108	0.0015	−0.0071
Zn	0.4619	0.7420	0.6451	0.0082	−0.0085	−0.0076	0.0054	−0.0058	−0.0063
Zn	0.7753	0.2581	0.9704	0.0174	0.0096	−0.0103	0.0167	0.0073	−0.0078
Zn	0.4619	0.2420	0.6451	0.0082	−0.0089	−0.0076	0.0058	−0.0065	−0.0068
Zn	0.7753	0.7581	0.9704	0.0184	0.0093	−0.0102	0.0169	0.0077	−0.0078
Zn	0.1626	0.1456	0.8995	−0.0138	0.0023	−0.0049	−0.0116	0.0017	−0.0029
Zn	0.0745	0.8544	0.7160	0.0075	0.0052	−0.0084	0.0062	0.0035	−0.0065
Zn	0.1626	0.6456	0.8995	−0.0082	−0.0014	0.0097	−0.0066	−0.0010	0.0087
Zn	0.0745	0.3544	0.7160	0.0178	−0.0032	−0.0106	0.0180	−0.0023	−0.0086
Zn	0.9049	0.9528	0.9620	−0.0139	0.0041	−0.0046	−0.0112	0.0019	−0.0027
Zn	0.2552	0.8506	0.8976	0.0071	0.0038	−0.0076	0.0060	0.0034	−0.0069
Zn	0.3322	0.0473	0.6534	−0.0075	−0.0028	0.0112	−0.0068	−0.0014	0.0087
Zn	0.9819	0.1494	0.7178	0.0187	−0.0036	−0.0104	0.0178	−0.0021	−0.0081
Zn	0.9049	0.4528	0.9620	−0.0152	0.0059	0.0148	−0.0101	0.0045	0.0123
Zn	0.2552	0.3506	0.8976	−0.0113	0.0079	−0.0057	−0.0105	0.0058	−0.0032
Zn	0.3322	0.5473	0.6534	−0.0066	−0.0065	−0.0086	−0.0057	−0.0038	−0.0064
Zn	0.9819	0.6494	0.7178	−0.0078	−0.0082	0.0123	−0.0054	−0.0057	0.0097
Zn	0.6169	0.0569	0.9557	−0.0124	0.0062	0.0159	−0.0106	0.0035	0.0111
Zn	0.5733	0.8234	0.8086	−0.0107	0.0091	−0.0078	−0.0091	0.0062	−0.0032
Zn	0.6203	0.9432	0.6597	−0.0064	−0.0077	−0.0087	−0.0050	−0.0032	−0.0056
Zn	0.6638	0.1767	0.8069	−0.0072	−0.0087	0.0117	−0.0057	−0.0061	0.0098
Zn	0.6169	0.5569	0.9557	0.0042	−0.0054	−0.0037	0.0001	−0.0036	0.0009
Zn	0.5733	0.3234	0.8086	−0.0158	0.0063	0.0075	−0.0130	0.0035	0.0061
Zn	0.6203	0.4432	0.6597	0.0031	−0.0067	−0.0023	0.0004	−0.0033	0.0007
Zn	0.6638	0.6767	0.8069	−0.0162	0.0066	0.0078	−0.0130	0.0036	0.0063

tions are very time-consuming, and the goal of the present study is to establish trends in crystal morphology, we do not explicitly consider the effects of atomic relaxation on the surfaces in the subsequent calculations. From the above discussion, we regard four-layer slabs (8 iron and 104 zinc atoms) as the minimum thickness (about 23.5 Å) needed to obtain meaningful results.

C. Morphological prediction and comparison with empirical method calculations

The external morphology of crystalline materials from the internal crystal structure can be predicted by using three methods. The BFDH method is based on geometrical considerations. The attachment energy and surface energy method are via the attachment and surface energy, respectively. These energies can be obtained by using various empirical techniques based on interatomic potentials or *ab initio* method. In this section, we systematically compare the crystal morphology the of $FeZn_{13}$ system predicted by using

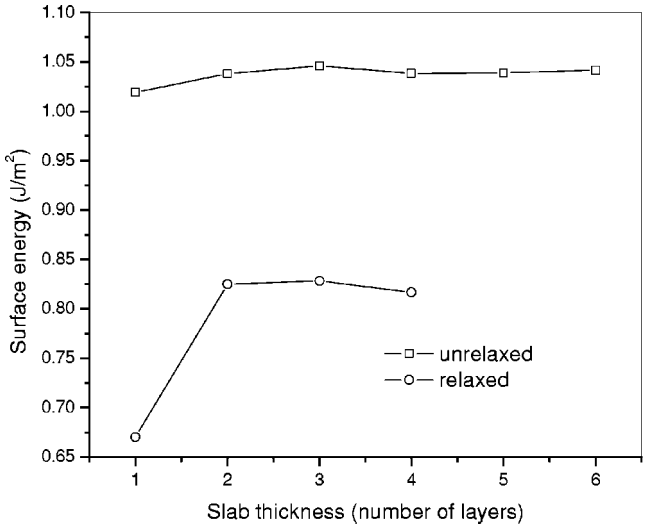

FIG. 4. The evolution of surface energy with increasing slab thickness.

TABLE IV. Calculated center-to-face distances D(Å) by using the BFDH method, attachment energies E_{att}(kJ/mol) and surface energies E_{surf}(J/m^2) by using force field energy and DFT method, and relative growth rates (R) for different Miller index (hkl) five-layer slab faces of $FeZn_{13}$.

(hkl)	BFDH method		Attachment energy method				Surface energy method			
			Force field		DFT		Force field		DFT	
	D	R	E_{att}	R	$E_{att}/10^4$	R	E_{surf}	R	E_{surf}	R
(110)	16.138	1.000	−27.527	1.000	−5.775	1.004	−0.0347	1.038	1.038	1.414
(001)	20.097	1.245	−31.812	1.156	−5.780	1.005	−0.0327	1.000	1.103	1.501
(200)	18.728	1.160	−32.319	1.174	−5.751	1.000	−0.0354	1.085	0.735	1.000
$(20\bar{1})$	24.843	1.539	−41.923	1.523	−5.819	1.012	−0.0356	1.092	1.580	2.151
$(11\bar{1})$	24.405	1.512	−41.452	1.506	−5.816	1.011	−0.0358	1.096	1.552	2.113
(111)	27.075	1.678	−46.391	1.685	−5.846	1.017	−0.0366	1.121	1.925	2.621
(020)	26.288	1.629	−44.573	1.619	−5.771	1.003	−0.0359	1.100	0.742	1.010
(201)	29.867	1.851	−49.523	1.799	−5.828	1.013	−0.0360	1.102	1.691	2.303

these methods. The faces which are likely to appear in the morphology need to be determined first so that the following calculations can be performed on them. The BFDH method was used to create several low Miller index surfaces of $FeZn_{13}$ studied here. The calculated results are given in Table IV.

The order of morphological importance predicted by the BFDH method is:

$$(110) > (200) > (001) > (11\bar{1}) > (20\bar{1}) > (020) > (111) > (201).$$

It is found that the (110), (200), and (001) surfaces have the most morphological importance. At the empirical level, the attachment energy method has predicted the following ordering of the morphological importance:

$$(110) > (001) > (200) > (11\bar{1}) > (20\bar{1}) > (020) > (111) > (201).$$

The prediction that most stable three surfaces are (110), (001), and (200) agrees with that by the BFDH method, but the relative sequence found for (001) and (200) disagrees with the BFDH predictions. The surface energy method based on the empirical level has determined the order of the surface stability:

$$(001) > (110) > (200) > (20\bar{1}) > (11\bar{1}) > (020) > (201) > (111).$$

The results also show that the (001), (110), and (200) surfaces have the most morphological importance. From the calculated results, we find that all the BEDH method, the attachment energy and surface energy method based on the empirical level have predicted that the (001), (110), and (200) surfaces have the most morphological importance, but the relative sequence found for (001), (110), and (200) is different at three methods.

At the DFT level, the attachment energy method has predicted the following ordering of the morphological importance:

$$(200) > (020) > (110) > (001) > (11\bar{1}) > (20\bar{1}) > (201) > (111).$$

The surface energy method based on the DFT level has determined the order of the surface stability:

$$(200) > (020) > (110) > (001) > (11\bar{1}) > (20\bar{1}) > (201) > (111).$$

The results show that the attachment energy and surface energy method based on the DFT level have presented the same order of the morphological importance for eight low-index surfaces of $FeZn_{13}$ system, and the (200), (020), and (110) are most stable three surfaces.

Although the order of the morphological importance predicted at DFT level are different from that at the empirical technique, they both present that the (200) and (110) are more stable surfaces. The BFDH method also draws the same conclusion. Compared with DFT, various empirical techniques based on interatomic potentials highly depend on the quality of the interatomic potentials, but they can be applied to larger crystals and especially geological specimens. The BFDH method is an approximation, and takes no account of the details structure or energetics of a crystal. The stronger the bonding effects in the crystal, the less accurate the method becomes. In many cases, however, one can get good approximations, and the method is always useful for identifying important faces in the growth process. The crystal morphology derived by the attachment energy method is the growth morphology. For larger systems, the growth morphology has been found to best reproduce the experimental results. The attachment energy model assumes that the surface is a perfect termination of the bulk and that no surfaces relaxation takes place. The surface energy method can be used to predict the equilibrium morphology. The equilibrium

morphology has been found to agree well with small experimentally grown crystals less than a micron in diameter.[28,29]

D. Equilibrium crystal shape

The equilibrium crystal shape can be obtained by minimizing the total surface free energy for a fixed crystal volume.[30] At $T=0$ K, the equilibrium crystal shape is completely determined by the anisotropy of the surface energy.[31] Hence, in the case of weak anisotropy, the equilibrium crystal shape is a sphere, while in the case of strong anisotropy it may be a complicated polyhedron.

The equilibrium crystal shape may be determined by the Wulff construction,[32] which assumes a complete knowledge of the orientation dependence of the surface energy. According to the procedure of the Wulff construction, a polar plot of surface energy is made. A vector whose length is equal to the surface energy in this orientation is chosen and then a plane perpendicular to the vector is drawn, passing through the tip of the vector. The inner envelope of all these planes gives the equilibrium shape of a crystallite under ideal conditions. Crystal planes that are part of this construction are thermodynamically stable.

The experimental measurement of equilibrium crystal shapes is difficult because it is not reach true equilibrium, moreover, it has not been possible to make the measurement for a wide range of materials. First-principles method can be used to predict the orientation dependence of the surface energy and to determine the $T=0$ K, the equilibrium crystal shape. In order to evaluate the energies of metal surfaces as a function of orientation, Wei and Chou[31] have proposed a cluster expansion of the total energy based on a limited number of low-index surface energies obtained from first-principles calculations. In the present application of the Wulff construction for these $FeZn_{13}$ surfaces, we have used the surface energies calculated from DFT and also from a cluster expansion of the total energy.

In a cluster expansion one expresses the total energy of a given crystal as linear combination of one-site, two-site, and higher interatomic potentials.[33] For transition metal surfaces, a cluster expansion of the total energy needs only to include pairwise interactions to describe the higher-index surfaces with reasonable accuracy.[31] We therefore use the following expansion of the surface energy[34,35]

$$E_{\mathrm{surf}}(hkl) \approx \sum_{s}^{N_s} n_s(hkl) V_s^{(2)}, \tag{4}$$

where $n_s(hkl)$ is the number of broken pair-bonds in the sth coordination-shell for a surface of index (hkl), $V_s^{(2)}$ the pair potentials of the sth shell, and N_s the number of coordination shells included in the expansion. In Table V, we compare the surface energies of several high-index surfaces obtained by the cluster expansion with the corresponding DFT results. Here we used $N_s=3$ which was found to yield sufficiently converged surface energies for most high-index surfaces of transition metals.[31,34] It can be seen from Table V that the surface energies for several surfaces from the cluster expansion are in agreement with DFT results. The neglect of three-body and higher interactions is expected to play a role only for early transition metals. When many coordination shells are considered in the pair-potential expansion, as in the present case, some of the neglected N-body terms are "renormalized" into the effective pair interactions and the accuracy becomes acceptable also for early transition metals.[31,34]

TABLE V. The surface energies (J/m^2) of several high-index surfaces calculated using the DFT method and the cluster expansion.

Method	(200)	$(20\bar{1})$	$(11\bar{1})$	(020)	(201)
DFT	0.735	1.580	1.552	0.742	1.691
Cluster expansion	0.746	1.632	1.594	0.761	1.745

In principle, the Wulff plot should be determined by the surface energy at all possible orientations. We have information of the orientation dependence of the surface energy for eight principle orientations only. This restriction is probably not a serious problem since for most of the generic models.[36] The equilibrium shape for $FeZn_{13}$ is shown in Fig. 5. Equilibrium crystal shapes of $FeZn_{13}$ constructed with surface energies calculated from DFT and from a cluster expansion of the total energy are both complicated polyhedrons. This

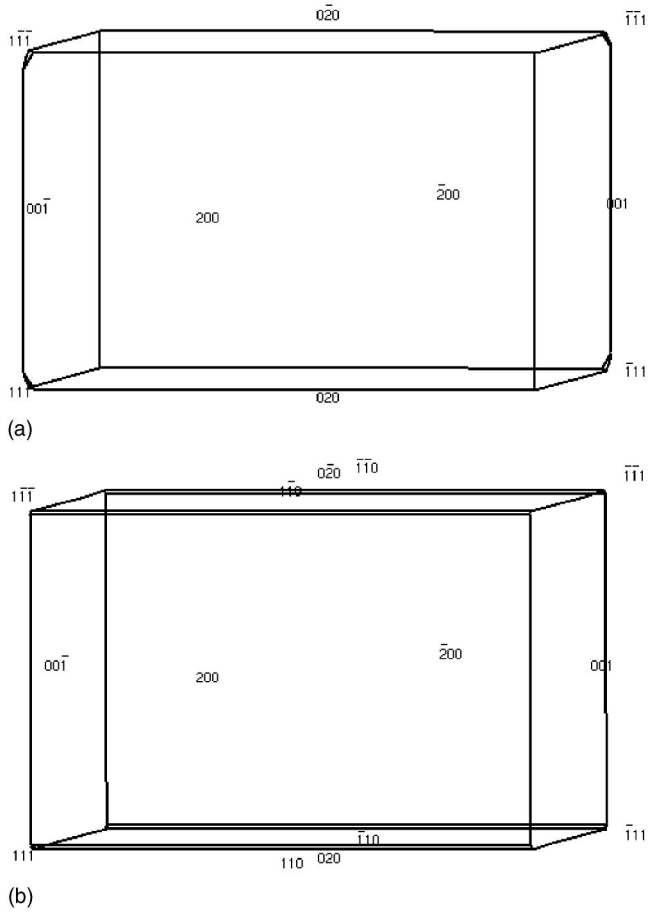

FIG. 5. Equilibrium crystal shapes of $FeZn_{13}$ constructed with surface energies calculated from DFT (a) and from a cluster expansion of the total energy (b).

shows that $FeZn_{13}$ exhibits a stronger anisotropy. Although the surface energies for the eight surfaces from DFT are in agreement with the cluster expansion results, the equilibrium crystal shape from these two approached is a little different. In Fig. 5(b), {110} facets appear on the equilibrium crystal shape, yet Fig. 5(a) does not expose the {110} facet. This is because surface energies of (200) and (020) surfaces from the cluster expansion are somewhat larger than that from DFT.

IV. CONCLUSIONS

In this study, we have performed periodic DFT total energy calculations to investigate the morphology of the $FeZn_{13}$ surfaces by using slab model. The effects of the slab thickness, the vacuum width between slabs and the surface relaxation on surface energy have been tested. The results show that as long as the vacuum width is 6 Å or more, the influence of vacuum width on surface energy is small. An approximately 23.5 Å thick slab is enough to obtain meaningful results. Relaxation of the slab surface has a small effect on surface structure. The order of the morphological importance predicted at the DFT level is $(200)>(020)>(110)>(001)>(11\bar{1})>(20\bar{1})>(201)>(111)$. We also present comparisons of the crystal morphology predicted by the BFDH, attachment energy and surface energy method at empirical and DFT level. The calculated surface energy anisotropies are then applied to the determination of the equilibrium shape of $FeZn_{13}$.

*Author to whom correspondence should be addressed. FAX: (65)-67780522. Email address: wuping@ihpc.a-star.edu.sg

[1] A. R. Marder, Prog. Mater. Sci. **45**, 191 (2000).
[2] O. Kubachewski and T. Massalski, *Binary Alloy Phase Diagrams* (ASM, Metals Park, OH 1986), p. 1128.
[3] K. Osinski, Doctoral thesis Technical University, Eindhoven 1983.
[4] G. Friedel, Bull. Soc. Fr. Mineral. **30**, 326 (1907).
[5] J. D. H. Donny and D. Harker, Am. Mineral. **22**, 446 (1937).
[6] P. Hartman and P. Bennema, J. Cryst. Growth **49**, 145 (1980).
[7] P. Hartman and W. Perdok, Acta Crystallogr. **8**, 49 (1955).
[8] H. M. Jin, Y. Li, and P. Wu, J. Mater. Res. **15**, 1791 (1999).
[9] P. Wu, H. M. Jin, and Y. Li, Chem. Mater. **11**, 3166 (1999).
[10] H. M. Jin, Y. Li, H. L. Liu, and P. Wu, Chem. Mater. **12**, 1879 (2000).
[11] G. Kresse and J. Hafner, Phys. Rev. B **47**, 558 (1993).
[12] G. Kresse and J. Hafner, Phys. Rev. B **49**, 14 251 (1994).
[13] G. Kresse and J. Furthmüller, Comput. Mater. Sci. **6**, 15 (1996).
[14] G. Kresse and J. Furthmüller, Phys. Rev. B **54**, 11 169 (1996).
[15] D. Vanderbilt, Phys. Rev. B **41**, 7892 (1990).
[16] G. Kresse and J. Hafner, J. Phys.: Condens. Matter **6**, 8245 (1994).
[17] J. P. Perdew and Y. Wang, Phys. Rev. B **45**, 13 244 (1992).
[18] J. P. Perdew, J. A. Chevary, S. H. Vosko, K. A. Jackson, M. R. Pederson, D. J. Singh, and C. Fiolhais, Phys. Rev. B **46**, 6671 (1992).
[19] B. P. Brown, Acta Crystallogr. **15**, 608 (1962).
[20] P. J. Gellings, E. W. de Bree, and G. Gierman, Z. Metallkd. **70**, 70 (1979).
[21] D. C. Cook and R. G. Grant, in *Galvatech'95 Conference Proceedings* (Chicago, 1995), p. 497.
[22] J. L. C. Daames, P. Villars, and J. H. N. van Vucht, *Atlas of Crystal Structure Types for Intermetallic Phases* (ASM International, Imprint Materials Park, OH, 1991).
[23] Z. Berkovitch-Yellin, J. Am. Chem. Soc. **107**, 8239 (1985).
[24] A. L. Rohl and D. H. Gay, J. Cryst. Growth **166**, 84 (1996).
[25] Cerius2, Molecular Simulations Inc., San Diego, 1997.
[26] J. E. Raynolds, J. R. Smith, G. L. Zhao, and D. J. Srolovitz, Phys. Rev. B **53**, 13 883 (1996).
[27] S. P. Bates, G. Kresse, and M. J. Gillan, Surf. Sci. **385**, 386 (1997).
[28] P. Hartman, Acta Crystallogr. **11**, 459 (1958).
[29] C. R. A. Catlow, S. C. Parker, and M. P. Allen, *Computer Modeling of Fluids, Polymers and Solids* (Kluwer, Dordrecht, 1990).
[30] G. Wulff and Z. Krist, Mineral. J. **34**, 449 (1901).
[31] S. Wei and M. Y. Chou, Phys. Rev. B **50**, 4859 (1994).
[32] M. C. Desjonquères and D. Spanjaard, *Concepts in Surface Physics* (Springer, Berlin, 1996).
[33] J. A. Moriarty and R. Phillips, Phys. Rev. Lett. **66**, 3036 (1991).
[34] L. Vitos, A. V. Ruban, H. L. Skriver, and J. Kollár, Surf. Sci. **411**, 186 (1998).
[35] L. Vitos, H. L. Skriver, and J. Kollár, Surf. Sci. **425**, 212 (1999).
[36] A. C. Shi, Phys. Rev. B **36**, 9068 (1987).